

Supplementary Information

Rheology and Structure of Elastic Capsule Suspensions within Rectangular Channels

Paul C. Millett

Department of Mechanical Engineering, University of Arkansas, Fayetteville AR 72701, USA
pmillett@uark.edu

1. Supplementary Movie Captions

Supplementary Movie 1: (left) Side and (right) head-on views of capsule suspension flow within a slit channel with $h/a = 5.1$, $Ca = 0.3$, and $Re = 10$.

Supplementary Movie 2: (left) Side and (right) head-on views of capsule suspension flow within a slit channel with $h/a = 5.1$, $Ca = 0.3$, and $Re = 400$.

Supplementary Movie 3: (left) Side and (right) head-on views of capsule suspension flow within a slit channel with $h/a = 1.8$, $Ca = 0.3$, and $Re = 2$.

Supplementary Movie 4: (left) Side and (right) head-on views of capsule suspension flow within a rectangular channel with $w/a = 10.1$, $h/a = 5.1$, $Ca = 0.3$, and $Re = 400$.

Supplementary Movie 5: (left) Side and (right) head-on views of capsule suspension flow within a rectangular channel with $w/a = 25.1$, $h/a = 5.1$, $Ca = 0.3$, and $Re = 400$.

2. Supplementary Figures

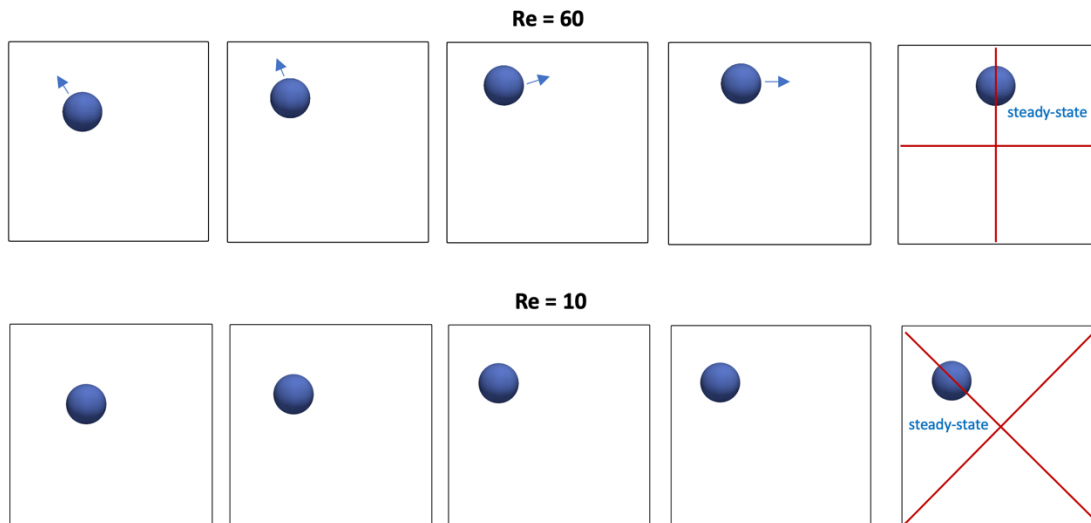


Figure S1: Snapshots of inertial lateral focusing for a single quasi-rigid particle ($Ca = 0.003$) in a square channel with $h/a = w/a = 5.1$ for: (top) $Re = 60$ and (bottom) $Re = 10$. The results show that the stable steady-state position is on main axes for $Re = 60$ and on the diagonal axes for $Re = 10$, in agreement with Schaaf and Stark [18] (note S&S used $Re = 100$ rather than $Re = 60$).

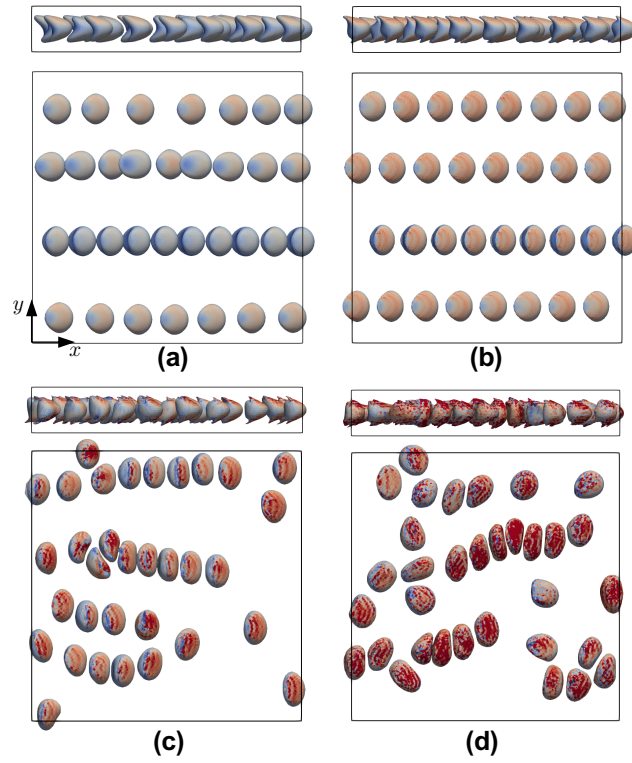


Figure S2: Capsule alignment in shallow slit channels ($h/a = 1.8$) for $Ca = 0.3$ and (a) $Re = 2$, (b) $Re = 10$, (c) $Re = 80$, and (d) $Re = 400$. Both side and top-down views are shown.

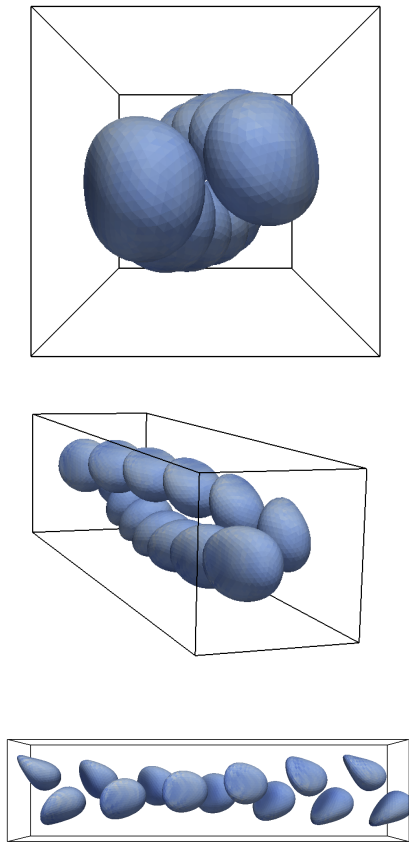


Figure S3: Simulation snapshots showing an example of double helical capsule assembly in a square channel ($h/a = w/a = 2.6$) with $Ca = 0.1$ and $Re = 100$. Once this structure formed, it would persist until the simulation was ended.

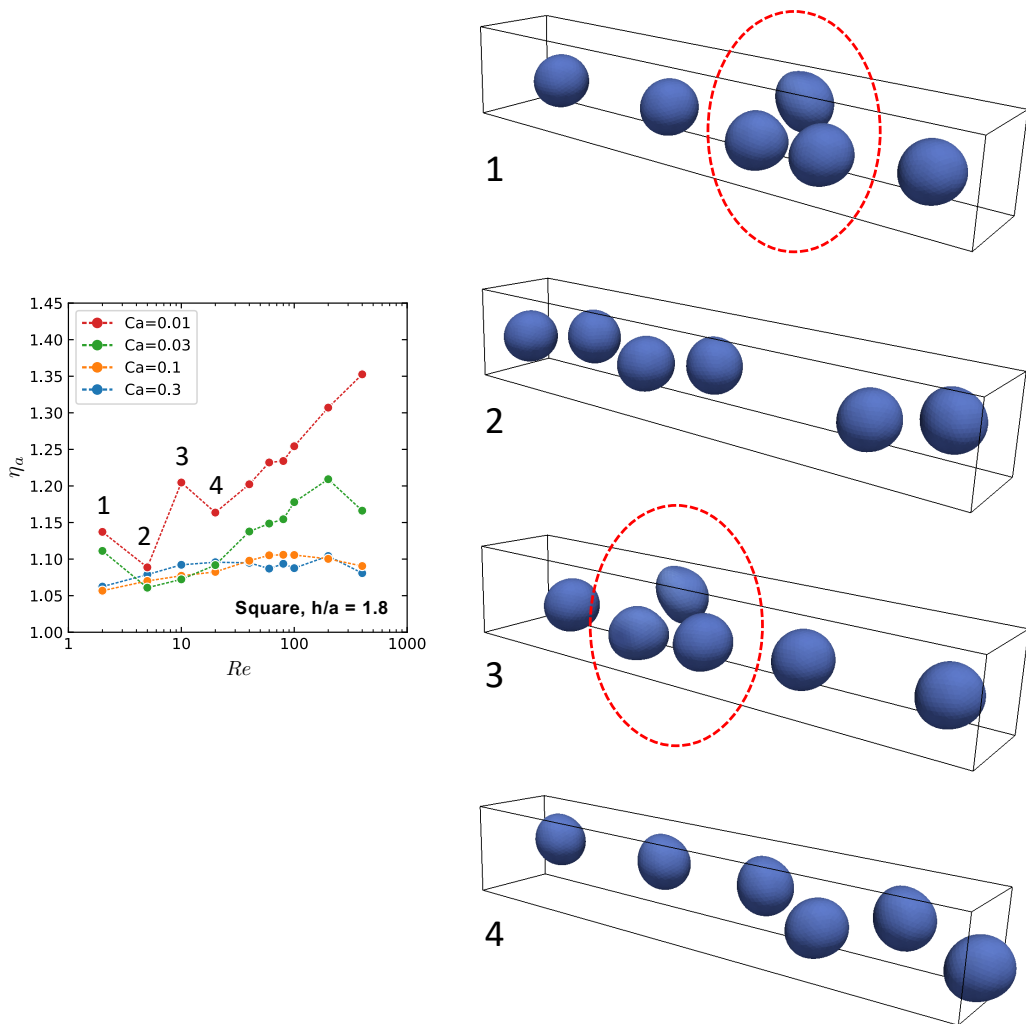


Figure S4: Capsule distributions in narrow square channels ($h/a = w/a = 1.8$) lead to variations in the apparent viscosity versus Re for the relatively rigid capsules ($Ca = 0.01$). For cases “1” and “3”, the formation of local regions with high capsule density results in higher values of apparent viscosity. All simulations are randomly initialized, and it was not clear if the formation of these high-density regions is also random or a consistent function of Re .

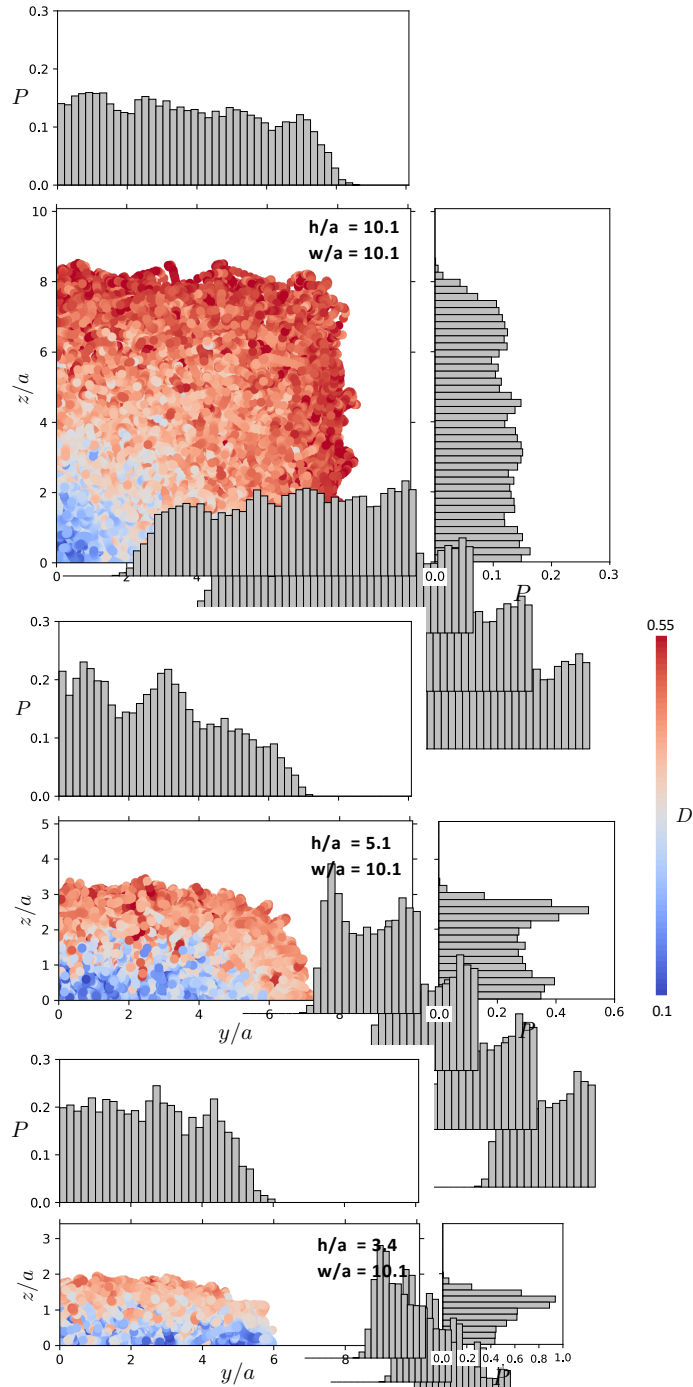


Figure S5: Scatter plots and histogram plots showing capsule distributions in rectangular channels with $Ca = 0.3$ and $Re = 400$. (Top) Square channel with $h/a = 10.1$ and $w/a = 10.1$. (Middle) Rectangular channel with $h/a = 5.1$ and $w/a = 10.1$. (Bottom) Rectangular channel with $h/a = 3.4$ and $w/a = 10.1$. All plots depict center-of-mass positions for capsules throughout the production time window for the simulations. The scatter plots are colored according to the Taylor deformation parameter, D . The histogram plots show a probability density, with the area under the curve equal to unity. These plots reinforce the conclusion that, for rectangular channels with aspect ratio not equal to one, a higher degree of inertial focusing occurs in the dimension that is greater in length (here, the y -direction).

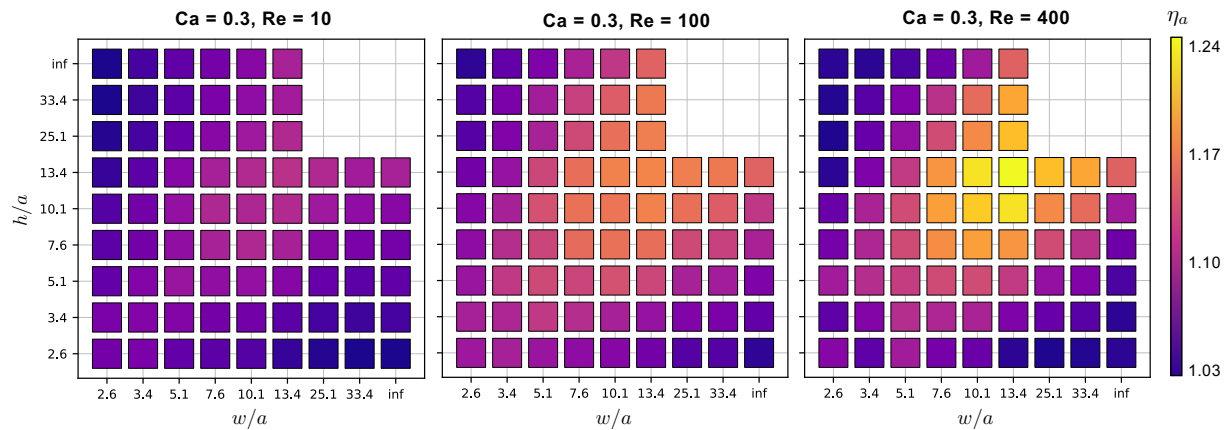


Figure S6: Apparent viscosity for the various channel cross-sectional dimensions for $Ca = 0.3$ and $Re = 10$ (left), 100 (center), and 400 (right). The apparent viscosity is highest along the $h = w$ diagonal associated with square channels. Increasing the channel aspect ratio by holding one channel dimension fixed and increasing (or decreasing) the other dimension results in a decrease in apparent viscosity.

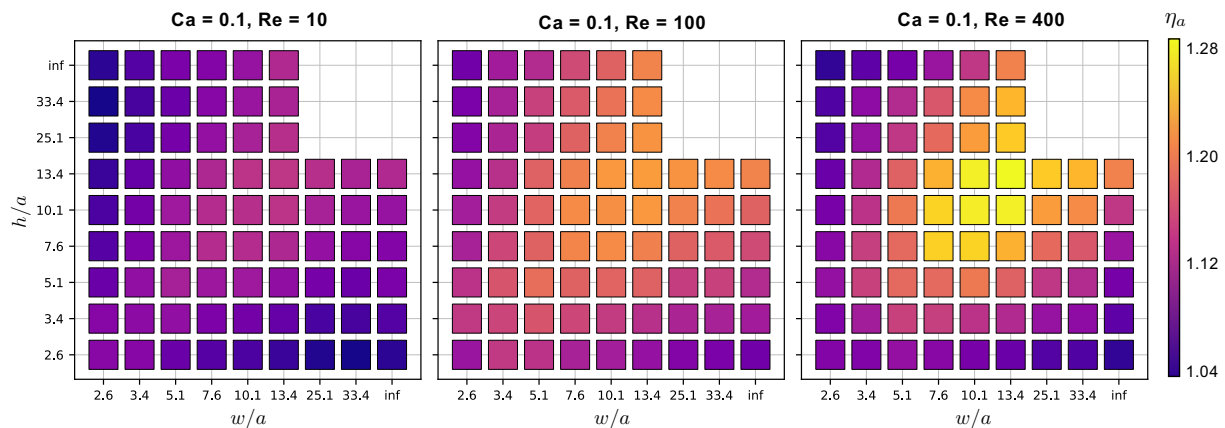


Figure S7: Apparent viscosity as a function of channel cross-sectional dimensions for $Ca = 0.1$ and $Re = 10$ (left), 100 (center), and 400 (right). The trend is similar to $Ca = 0.3$ (Fig. S6), but due to the slightly stiffer capsules here, the apparent viscosities are slightly higher (note the difference in colorbar scale).

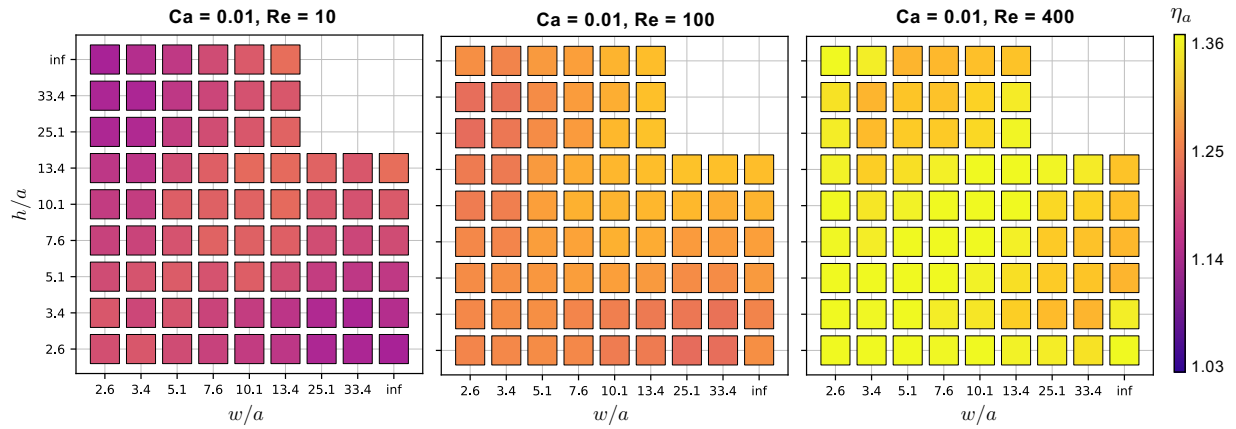


Figure S8: Apparent viscosity as a function of channel cross-sectional dimensions for $Ca = 0.01$ and $Re = 10$ (left), 100 (center), and 400 (right). Here, the capsules are relatively stiff, and the variation in apparent viscosity is much less with changing channel dimensions for a given Re .